THE APPLICATION OF FEM-EMA CORRELATION AND VALIDATION TECHNIQUES ON A BODY-IN-WHITE

Marc Brughmans
Jan Leuridan

LMS International
Interleuvenlaan 68
3001 Leuven, Belgium

Kevin Blauwkamp

GM - Saturn Corporation
1450 Stephenson Hwy.
Mail Drop #31
Troy, MI 48083

ABSTRACT

The paper reviews the application of FEM - EMA correlation and validation techniques to a body-in-white, namely the 1991 GM Saturn four door Sedan. The FEM model of this car consisted of 46830 dof's (half model). A multi-point experimental modal analysis (EMA) survey was executed for 360 response dof's. Classical techniques for correlation analysis such as MAC are applied. The paper introduces as well a variation of the MAC calculation that enables a better identification of regions of difference between FEM and EMA. Error localization methods have been applied to identify the regions of the FEM model causing most of the discrepancies between FEM and EMA. A FEM model updating procedure was executed to reduce the difference between FEM and EMA to acceptable limits.

1. INTRODUCTION

In the past decades numerous papers have been published on the verification of FEM models using measured data. Normal mode parameters are most commonly used as a comparison basis to describe the discrepancies between the analytical (FEM) and test (EMA) model. Model updating procedures are conceived to adjust FEM models so that the updated modal parameters better fit the experimental modal results. Most of the updating procedures can be classified either as a one step, non-iterative method or as an iterative method based on a sensitivity formulation [1]. The last approach yielding physically relevant and interpretable results is preferable to the direct matrix approach where individual stiffness and mass matrix elements can alter without any relation to the physical model from which they originate.

2. UPDATING OF LARGE FEM MODELS

Although some powerful iterative techniques have been developed in recent times to increase the interpretability and controllability of the updating process some negative characteristics still limit the applicability of these methods when large, complex FEM models are confronted with real measured data. First of all, the selectable parameters of the updating procedures correspond to physical FEM model attributes. In the modelization of complex structures such as a car body many idealizations (geometry, material properties, joints) have to be made resulting in error sources which can not be identified. In such a situation the required modal state may still be achieved by FEM model updating techniques but the modified FEM model will not reveal the real error source. Even in the case where all errors are caused by wrongly specified FEM input data, the success of the updating procedure will strongly depend on the selection of design parameters the analyst assumes to be wrong.

Furthermore typical incompatibilities between FEM and test models such as the mismatch in model size impose severe restrictions on model updating techniques that are based on orthogonality conditions. Indeed when measuring less than a half percent of the total number of FEM dofs, the expansion of test vectors (or the condensation of FEM matrices) can hardly be justified. Another incompatibility arises from the fact that usually complex modes are identified during a modal survey. Comparison with FEM normal modes necessitates transformation techniques to convert the complex test modes into real valued vectors ([2],[3]). These mode shape coefficients can be included as target parameters of the updating process when assuming a high quality EMA curve fit, a high one to one correlation between EMA and FEM modal vectors, a correct (FEM compatible) scaling of the test vectors and negligible transformation effects. The above mentioned restrictions can lead to a too limited set of target parameters in the updating process so that no unique solution can be guaranteed. In such situations input of the analyst on possible error locations are essential. Error localization methods complement the intuition of the analyst in the identification of these error regions. In the following application such an error localization method is presented together with a new analysis technique for better identification of discrepancies between correlated modal vectors.

3. APPLICATION SET-UP

3.1 Introduction

The structure under analysis is the body-in-white of the 1991 Saturn four door Sedan; see Figure 1.

3.2 FEM Model

The analytical dynamic characteristics of the body-in-white were predicted using an MSC/NASTRAN FEM model. Taking advantage of symmetry, only the right hand side of the

structure was modeled, with both symmetric and anti-symmetric boundary conditions being applied to the centerline grids of the model. Figure 2 gives a general overview on the FEM model.

Thin shell elements, QUAD4 and TRIA3, were used to model the physical parts of the body. Floorbeads, stiffening ribs, and associated parts were modeled with BAR elements. Spot welds that connected individual parts were simulated with RBE2 elements. A summary of the MSC/NASTRAN model attributes is given in Table 1.

MSC/NASTRAN Model Attributes		Number
	QUAD4	5421
	TRIA3	1365
Elements	BAR	160
	RBE2	1390
Nodes	GRID	7805
Materials	MAT1	164
Properties	PBAR	11
	PSHELL	82

Table 1. MSC/NASTRAN Model Attributes of SATURN body-in-white spaceframe

Solving this dynamic model yielded 8 symmetric and 9 anti-symmetric normal modes in the 0 - 75 Hz frequency range of interest.

3.3 Test Model

To quantify the dynamic characteristics of a production body-in-white and verify the dynamic prediction of the finite element model, an experimental modal analysis (EMA) survey was performed.

The body was supported by four air bladder isolators to approximate a "free-free" boundary condition for the test.

The body was excited with two electro-mechanical shakers using a burst random excitation technique. The frequency range of interest was 100 Hz. Frequency response function (FRF) data were obtained at 360 measurement degrees of freedom using 120 piezo-electric accelerometers. Figure 3 illustrates the measurement geometry of the test structure using a wire frame model representation. Exciter locations are identified with arrows.

The modal parameters of the body were obtained using the complete set of measurement FRF's and a least squares complex exponential parameter estimation technique. A total of 34 significant measurement modes were obtained in the 0 - 100 Hz frequency range.

3.4 Data Transfer

Both dynamic models were transferred to the database of CADA-LINK, a product for FEM-EMA correlation analysis. Interfacing to MSC/NASTRAN was realized through an OUTPUT2 file. Measured data was extracted from a CADA-MODAL database.

4. CORRELATION ANALYSIS

4.1 Test/Analysis Geometrical Correlation

A first requirement when dealing with large scale FEM and EMA models is the disposal of efficient data management tools to store the vast amount of analytical and experimental data in a coherent format, to build appropriate display models for simultaneous visualization of test and analysis results and to organize the FEM model in logical entities on which FEM -EMA correlation and updating techniques will operate. An important aspect in the compatibility phase is the identification of FEM dofs that have been measured. To this purpose the complex FEM geometry is compared with the test wire frame model. Based on four graphically correlated nodes, the experimental coordinate system was positioned in the analytical one with 3 translations, 3 rotation angles and a length scale factor. Checks were also made for missing (e.g rotational) dofs and incompatible nodal coordinate systems. Figures 4 and 5 show how the test wire frame model of the full car is fitted to the FEM model of the half car. Recovering the common dofs between FEM and EMA the test modal vectors were transformed to the FEM analysis system. A second geometrical correlation analysis was performed with a mirrored FEM geometry model. Not the whole FEM model was mirrored but only a wire frame model generated from the set of connections between previously correlated test nodes. The mirror action was also executed on the FEM modal vectors restricted to the common FEM and EMA dofs. After correlation with the test wire frame model, the comparison between these reduced FEM modal vectors of the full car and the test mode shapes could be started.

4.2 Test/Analysis Modal Correlation

Modal Correlation using the MAC Criterion

The anti-symmetrical and symmetrical FEM mode shapes were merged in one modal database and correlated with the test mode shapes using the Modal Assurance Criterion (MAC) technique. The MAC matrix correlating the 17 FEM modes with the first 20 test modes is visualized in Figure 6. From this MAC matrix the mode pairs with the highest MAC value were extracted (excluding the rigid body modes). They are listed in Table 2 and visualized in Figures 7 and 8 with a frequency error chart and a 2D frequency graph.

Original FEM Frequency (Hz)	EMA Frequency (Hz)	diff Hz	diff %	MAC
27.277	25.419	-1.859	-6.8	0.867
28.513	28.631	0.117	0.4	0.905
42.051	42.025	-0.027	-0.1	0.810
49.408	43.318	-6.089	-12.3	0.661
51.833	52.376	0.543	1.0	0.556
55.998	57.340	1.342	2.4	0.446
61.631	59.797	-1.834	-3.0	0.239
62.054	61.221	-0.833	-1.3	0.412
64.424	61.421	-3.003	-4.7	0.399
68.959	66.742	-2.217	-3.2	0.503
71.373	69.249	-2.123	-3.0	0.797

Table 2. Frequency comparison of original FEM and EMA dynamic models.

Five mode pairs show a correlation with a MAC higher than 0.65. Figure 9 illustrates one of them. A very low correlation (0.239) is also observed in the correlation table. The FEM mode shape (Figure 10) shows a very local deformation of the car. With the exciter located in front of the car (Figure 3) it is not likely to extract this pure local mode. The other correlations have a 0.4-0.55 MAC level, Differences in mode shape behavior between these correlated mode pairs can be observed in an animated display but no conclusions can be drawn explaining which regions of differences are causing the low MAC value.

MAC Variation Technique

Starting point of the method is the definition of the Modal Assurance Criterion (MAC), [4] correlating two vectors X and Y of vector length N :

$$MAC^{N}_{(X,Y)} = \frac{(\{X_N^T\}\{Y_N\})^2}{\{X_N^T\}\{X_N\}\{Y_N^T\}\{Y_N\}} \quad (1)$$

Significant modal vector discrepancies have a negative or zero contribution to the vector product of the denominator. Typically these discrepancies correspond to an anti-phase behavior between the two vectors or a local deformation observed in one mode and not in the other one. These differences are identified with a procedure evolving over several steps (S = 1,N-1). In each step a dof will be identified that influences the MAC value the most in negative way :

1. Construct subvectors $X_{N-(S-1)}$ and $Y_{N-(S-1)}$ by excluding the dofs identified in the previous steps.

2. for each of the remaining dofs $MAC_{(X,Y)}$ is calculated with subvectors X_{N-S} and Y_{N-S} obtained by excluding the dof under analysis from the subvectors of step 1.

3. the dof that will be retained in step S is the one with the highest MAC value calculated in step 2.

4. exclude this dof from $X_{N-(S-1)}$ and $Y_{N-(S-1)}$ and calculate vector lengths $\|X_{N-S}\|$ and $\|Y_{N-S}\|$.

At the end an ordered list of dofs is obtained with three values associated to each of them. The first one is the MAC value obtained by excluding the actual dof and the dofs of the previous steps from the MAC analysis. The two other values are the vector lengths of the subvectors so created. This information gives the analyst an idea on how much of the original motion must be excluded to obtain a certain MAC level. Local differences can have a strong influence on the global correlation value as illustrated in Figure 11 presenting the results of a MAC variation analysis on the correlated mode pairs shown in Figure 12. In this case the original MAC value of 0.55 can be raised to 0.72 by restricting the FEM and EMA vectors with respectively 5 and 2 percent. Rather than picking individual dofs the method identifies regions of modal vector discrepancies. A second illustration shown in Figures 13 and 14 compares a local FEM mode shape with a global EMA mode shape. In the MAC variation analysis first a region at the back of the car is identified where the FEM and EMA mode shapes are in anti-phase. Next, regions are identified were deformation is observed in the EMA mode shape but not in the FEM vector. The difference global versus local mode is indicated by the fact that a MAC level of 0.70 (originally 0.50) is obtained by removing 19 percent of the motion of the test vector and only 4 percent of the FEM vector.

4.3 Analysis Model Updating

Model Updating Approach

The updating technique used in the present application is based on a forward sensitivity formulation in which sensitivities of modal parameters to proportional changes of the FEM element matrices are applied ([5]) :

$$\underset{n\times 1}{\{q_t\}} = \underset{n\times 1}{\{q_s\}} + \underset{n\times N}{[S(\{p_s\})]}\ \underset{N\times 1}{\{dp\}} \qquad (2)$$

where,

$\{q_t\}$ represents the desired state of the n modal parameters

$\{q_s\}$ represents the current state of the n modal parameters

$\{p_s\}$ represents the current state of the N system variables that can vary during the updating process. These parameters are selected to be proportional to the element mass or stiffness matrix or to a group thereof.

$[S(\{p\})]$ is the matrix of sensitivity coefficients of the n modal parameters w.r.t the N system variables. [6]

Equation (2) is solved for parameter updates {dp} using a Bayesian parameter estimation scheme that allows the analyst to express his confidence in each of the target modal parameters and the current parameter state.

Definition of Model Updating Parameters.

An important aspect of the FEM model updating procedure is the appropriate choice of updating parameters. Elements of the half car FEM model with equal properties were processed into groups for which the stiffness or mass characteristics could vary as a whole. Some of the larger groups were split in smaller ones in order to have a more reasonable element distribution. A total of 106 groups were defined. They are visualized in Figure 2.

Error Localization based on a Sensitivity Approach

As the number of system variables (106 stiffness and mass parameters) largely exceeds the number of target responses (N = 212 >> n = 11 in equation (2)), it is not advised to apply the above updating procedure without locating the dominant errors in the model first. A method similar to the one proposed in [7] was used for this purpose. The principal idea behind this method is that it retains those columns of the sensitivity matrix that are best suited to represent the difference vector {d}:

$$\{d\} = \{q_t\} - \{q_s\} = [S_N]\{dp\} \tag{3}$$

The procedure progresses in successive steps and quite similar to the MAC variation analysis method. In each step (s) the subspace of the previous step is extended with one dimension. Among all possibilities the subspace is selected in which the difference vector { d } is described most accurately :

1. Construct submatrix $S_{[s-1]}$ with the columns of matrix S_N selected in the previous steps.

2. for each of the remaining columns parameter updates $\{dp_s\}$ are calculated by adding the column under analysis to S_{s-1}, yielding $S_{[s]}$ and solving equation (4) in a least square sense :

$$\{d\} = [S_s]\{dp_s\} \tag{4}$$

3. the error norm e is computed from the difference between the distance vector $\{ d \}$ and its representation $\{ d' \}$ in the subspace

$$\{d'\} = [S_s]\{dp_s\} \tag{5}$$

$$e = \|\{d\} - \{d'\}\| \tag{6}$$

4. the column yielding the smallest error norm e is retained

In order to prevent excessive deviation from the original state a Bayesian parameter estimation scheme was used to solve equation (4). With a global weighting factor the level of parameter updates was controlled. This way parameters with very low sensitivity values are excluded from the error identification process. As the dimension of the subspace is incremented during each step the representation of the distance vector improves and consequently the error norm is a non-increasing function of the number of steps. A typical function is shown in Figure 15. Each step (x-axis) in this figure is represented by the column that was selected in that step. Instead of the column number the parameter corresponding to the column is indicated with a group name and a parameter type (MASS or STIFFNESS). Most of the discrepancies between the FEM model and the structure are removed in the beginning of the process as the subspace grows relatively most in this phase. Dominant modeling errors are identified by the parameters which were first selected in the error localization process. After a number of steps the slope of the error norm function is small. Adding one more parameter to the already selected parameter set will not significantly contribute to a better representation of the distance vector. A second type of function shows the evolution of an individual parameter update as a function of the number of steps. A typical function is shown in Figure 16 where the evolution of the parameter selected in the first step of Figure 15 is visualized. For each step the vector of parameter updates can be visualized with a histogram. As an example the parameter updates at the last step of Figure 15 are shown in Figure 17. The results of the error localization procedure is conditioned by the

definition of the distance vector (the number of sensitivity equations), the definition of the updating parameters (group definitions) and the weighting of these parameters. The influence of weighting on the error identification process is presented with Figures 15-17 (medium weighting of parameters), Figures 18-20 (low weighting), and Figures 21-23 (high weighting). A low weighting factor yields a high quality result (small error norm in Figure 18) but the level of parameter updates is considerable high (Figure 20). A high weighting factor reverses this situation. A medium weighting factor yields a good compromise. (Figures 15-17). The error localization results of this case are also confirmed by the fact that most of the identified error parameters were also detected in the case with low weighting.

Analysis Model Updating

The dynamic model updating technique outlined in section 4.3.1 has been implemented in the LMS CADA LINK software package. A total of 212 system variables, described in section 4.3.2. was considered for the correction of the frequency discrepancy between 11 correlated mode pairs (section 4.2). The parameters identified with the error localization method (section 4.3.4) received a low confidence factor. After eight iterations the frequency alignment shown in Table 3 and Figures 7-24 was obtained. Frequency differences were limited to maximum 5 percent and the initial error norm was reduced with 75 %.

Updated FEM Frequency (Hz)	EMA Frequency (Hz)	diff Hz	diff %	MAC
25.388	25.419	0.031	0.1	0.915
28.545	28.631	0.085	0.3	0.880
41.377	42.025	0.647	1.6	0.805
44.495	43.318	-1.177	-2.6	0.673
51.587	52.376	0.789	1.5	0.460
56.805	57.341	0.537	0.9	0.552
59.727	59.797	0.069	0.1	0.373
60.421	61.221	0.800	1.3	0.351
62.174	61.421	-0.753	-1.2	0.369
66.833	66.742	-0.091	-0.1	0.518
69.257	69.249	-0.008	0.0	0.796

Table 3 Frequency comparison of Updated FEM and EMA dynamic models.

The updated parameters correspond to the ones identified with the error localization method.

5. CONCLUSIONS

The application of classical FEM-EMA correlation and validation techniques in a realistic industrial environment have been reviewed. When comparing the dynamic characteristics of large FEM models with the dynamic behavior observed on the test structure some of the classical correlation techniques such as mode shape expansion, FEM system matrix reduction techniques and orthogonality checks can not be applied anymore. Mode shape animation is a powerful tool for the observation of mode shape differences but can not quantify the effect of local differences on the overall correlation between two mode shapes. An approach is presented for the identification of the regions of differences between mode shapes. Based on a MAC variation technique the method highlights the important modal vector discrepancies and orders them according to their effect on the global correlation of the two vectors (MAC). Having identified dominant errors in the FEM model with an error localization technique a substantial reduction of the FEM-EMA frequency misalignment was obtained with a model updating technique based

on a forward sensitivity approach. Since the overall structure of the FEM model is preserved in this approach, it allows the analyst to interpret the updating results with his own engineering experience and intuition.

6. REFERENCES

[1] N. Roy, A. Girard, L. Bugeat and J. Bricaut, "A Survey of Finite Element Model Updating Methods," Proceedings of the International Symposium on Environmental Testing for Space Programmes - Test Facilities and Methods, ESTEC Noordwijk, June 1990.

[2] F. Lembregts and M. Brughmans, "Estimation of Real Modes from FRF's via Direct Parameter Identification", Proceedings of the Seventh International Modal Analysis Conference, Las Vegas, Nevada, 1989, pp. 631-636.

[3] M. Brughmans, F. Lembregts,"Using Experimental Normal Modes for Analytical Model Updating", Proceedings of the Eight International Modal Analysis Conference, Kissimmee, Florida, 1990.

[4] R. Allemang and D. Brown,"A Correlation Coefficient for Modal Vector Analysis", First International Modal Analysis Conference,Orlando,Florida, November 1982.

[5] J. Leuridan, M. Brughmans, W. Bakkers and A. De Landsheer,"FEM Model Correlation and Updating in a Heterogeneous Hardware and Software Environments", Proceedings of the 14th International Seminar on Modal Analysis, 11-15 Sept 1989, K.U.Leuven.

[6] H. Zeischka, O. Storrer, J. Leuridan "Calculation Of Modal Parameter Sensitivity Based On A Fem Proportionality Assumption", Proceedings of the Sixth International Modal Analysis Conference, Orlando, Florida, 1988.

[7] G. Lallement, J. Piranda and R. Fillod, "Recalage Parametrique par une Methode de Sensibilite", Proceedings of STRUCOME, Paris, 1988, p.979-1001

FIGURES

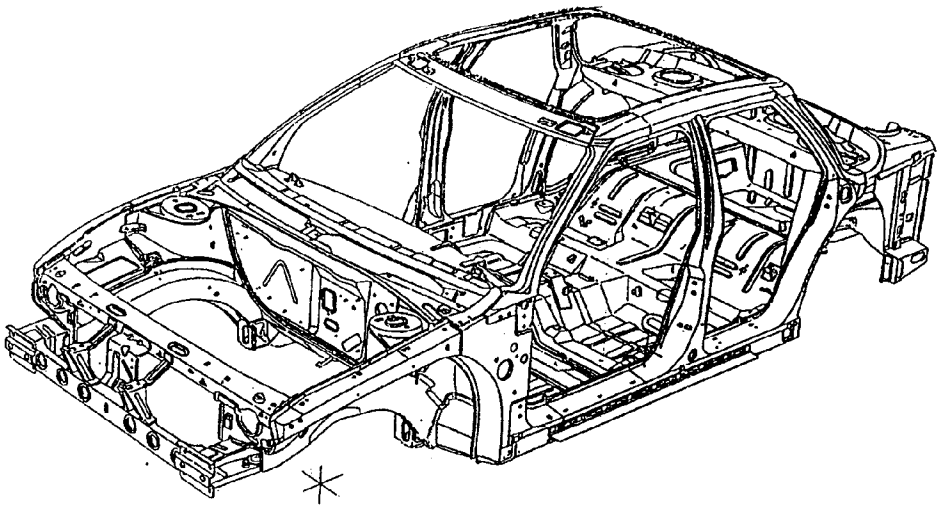

Fig. 1 : Saturn Sedan Body-in-White

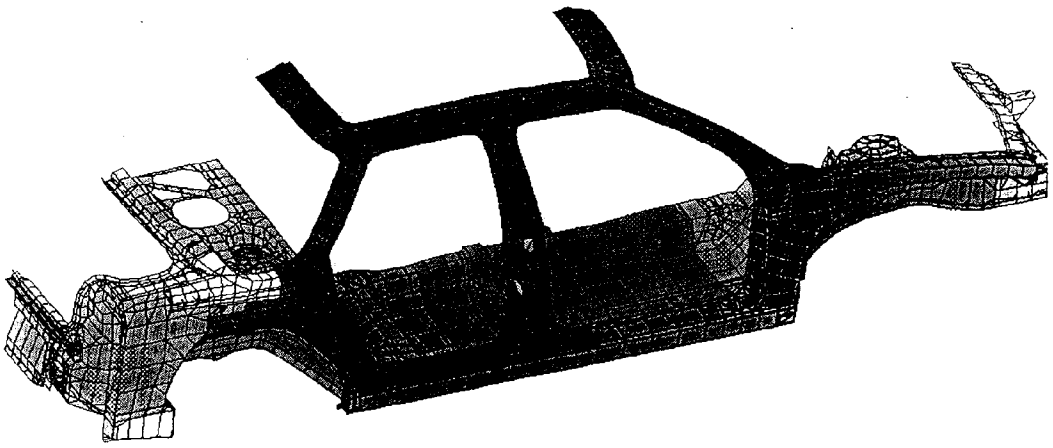

Fig. 2 : Saturn Sedan FEM Model

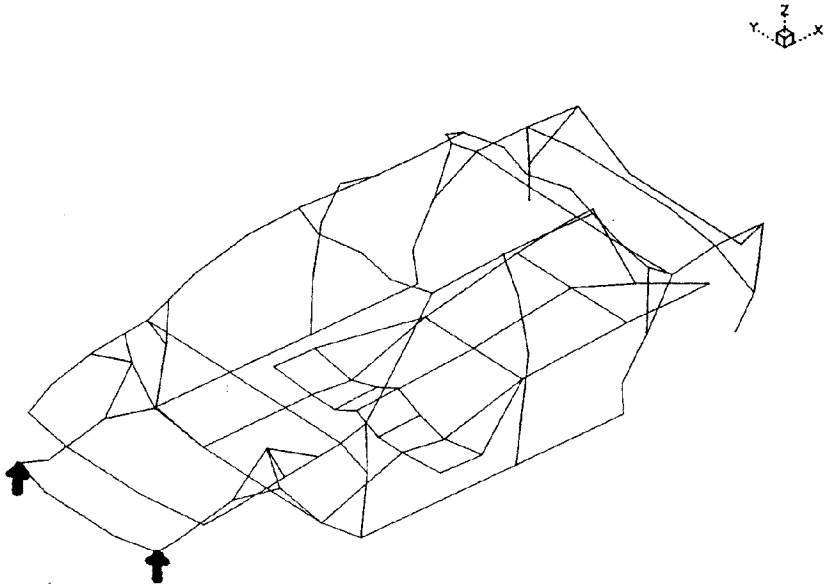

Fig. 3 : Saturn Sedan EMA Model

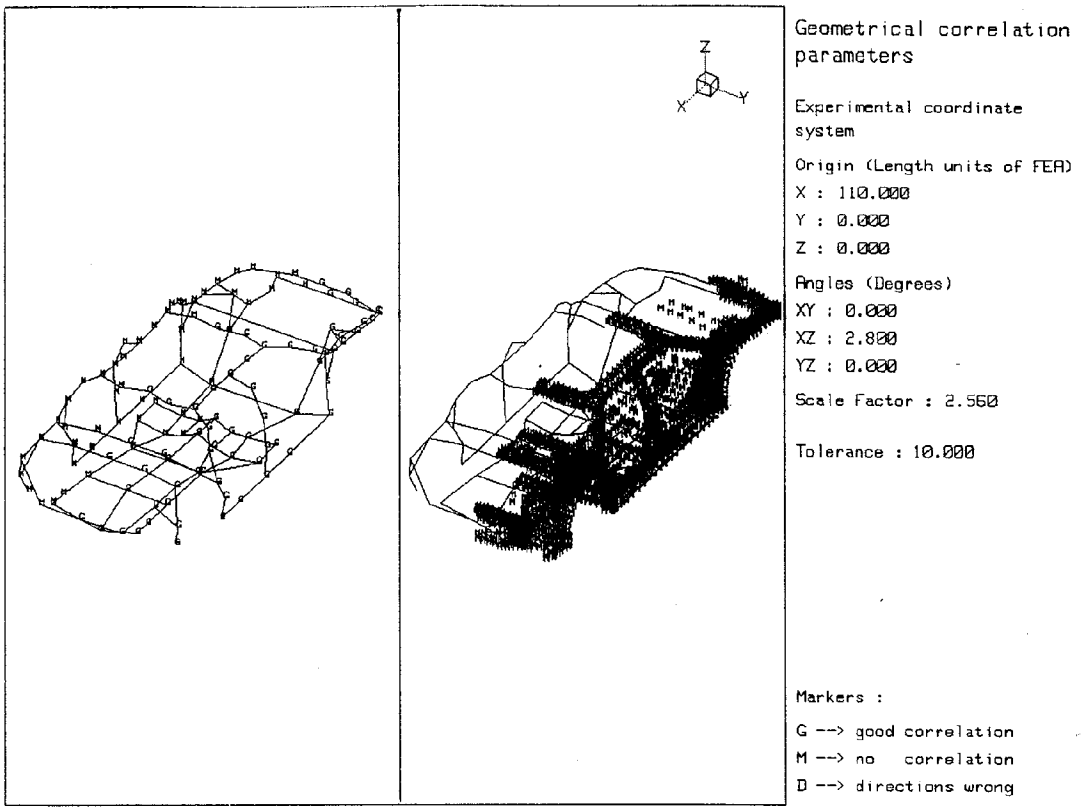
Geometrical correlation parameters
Experimental coordinate system
Origin (Length units of FEA)
X : 110.000
Y : 0.000
Z : 0.000
Angles (Degrees)
XY : 0.000
XZ : 2.800
YZ : 0.000
Scale Factor : 2.560
Tolerance : 10.000
Markers :
G --> good correlation
M --> no correlation
D --> directions wrong

Fig. 4

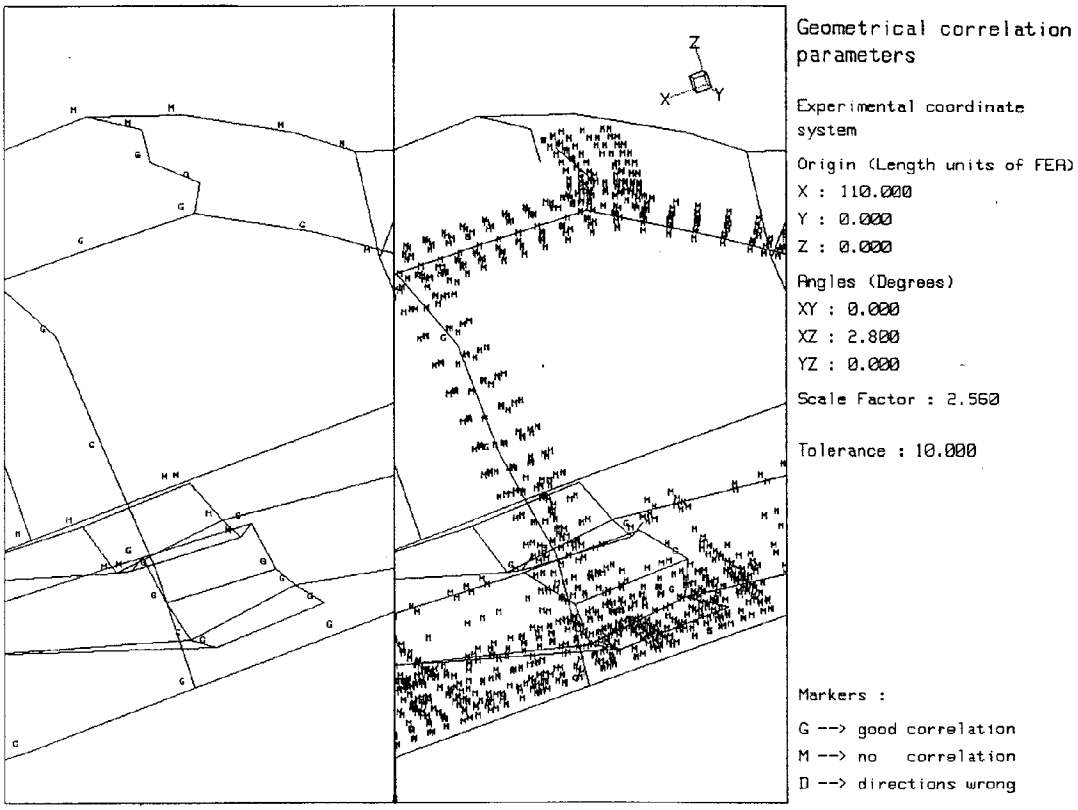
Geometrical correlation parameters
Experimental coordinate system
Origin (Length units of FEA)
X : 110.000
Y : 0.000
Z : 0.000
Angles (Degrees)
XY : 0.000
XZ : 2.800
YZ : 0.000
Scale Factor : 2.560
Tolerance : 10.000
Markers :
G --> good correlation
M --> no correlation
D --> directions wrong

Fig. 5

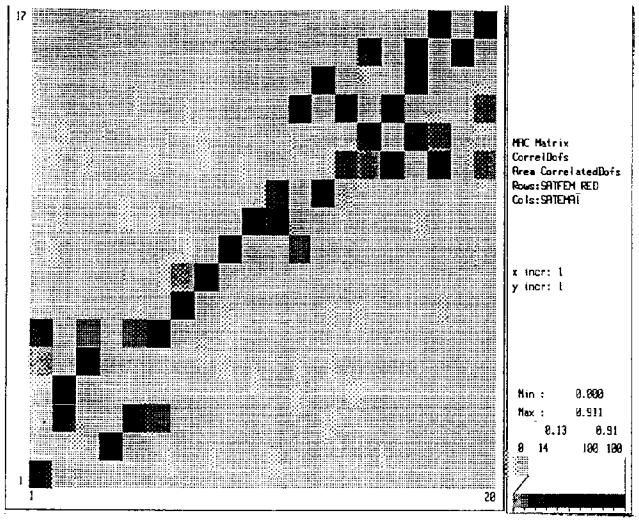

Fig. 6

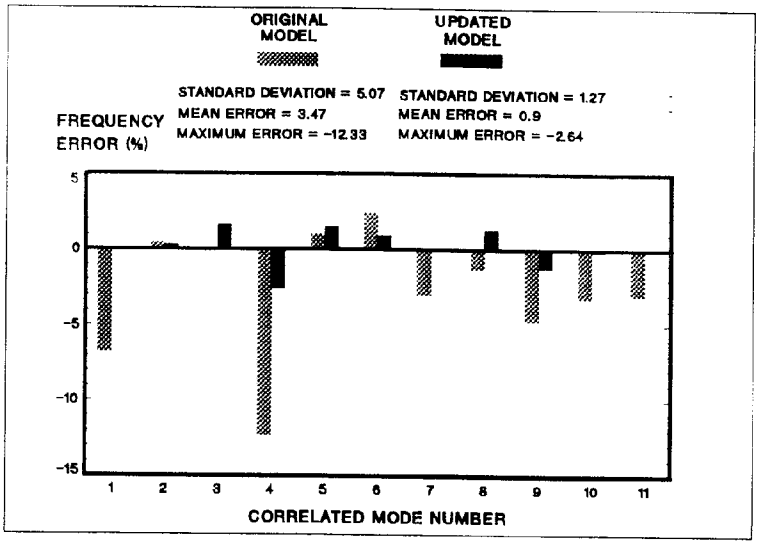

Fig. 7

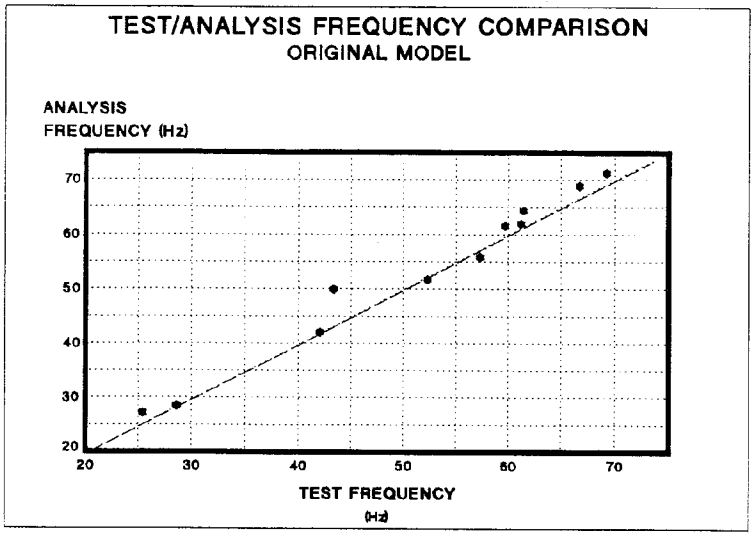

Fig. 8

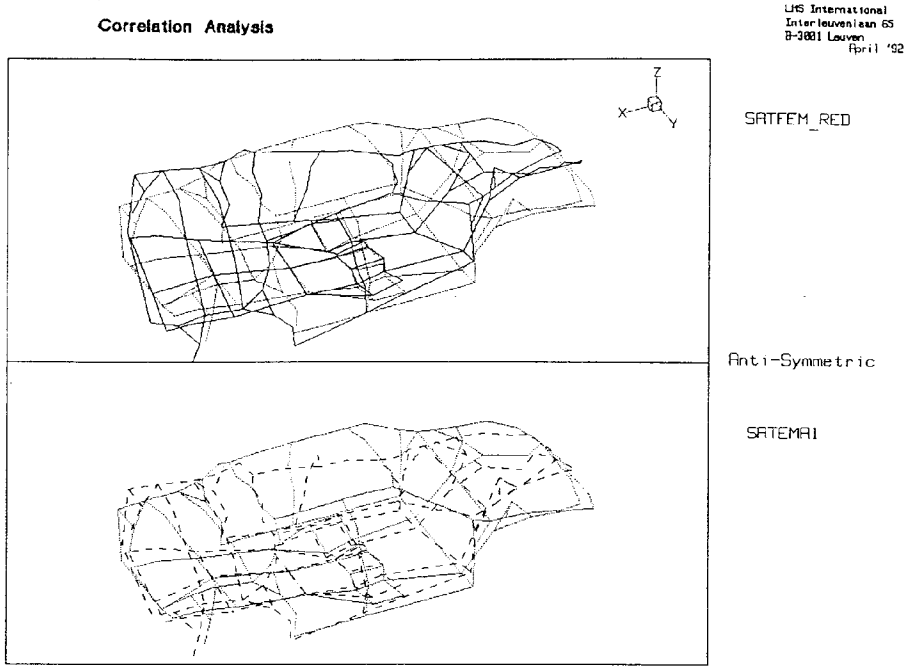
Correlation Analysis
LMS International
Interleuvenlaan 65
B-3001 Leuven
April '92
Z
X
Y
SATFEM_RED
Anti-Symmetric
SATEMA1

Fig. 9

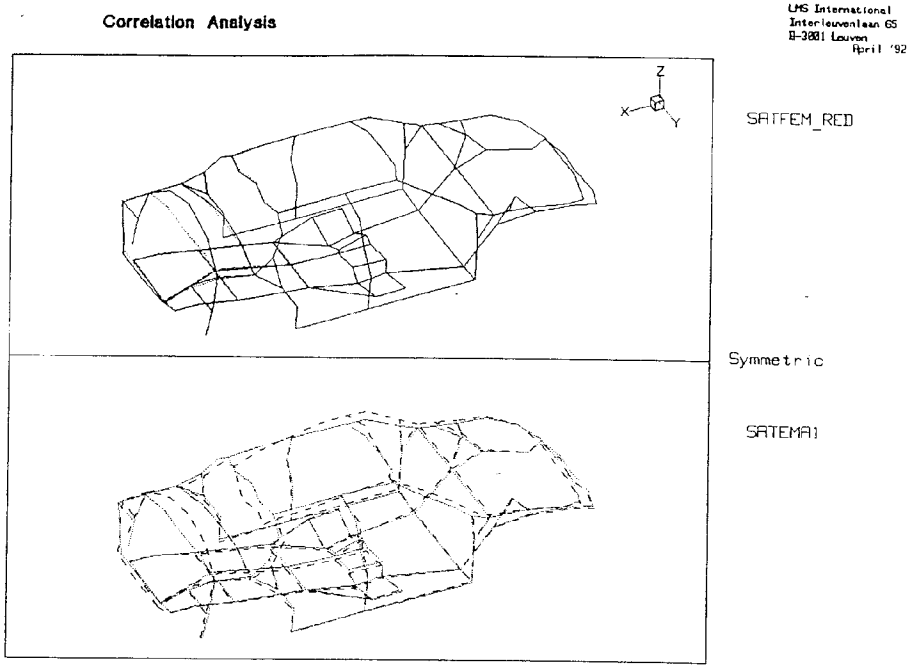
Correlation Analysis
LMS International
Interleuvenlaan 65
B-3001 Leuven
April '92
Z
X
Y
SATFEM_RED
Symmetric
SATEMA1

Fig. 10

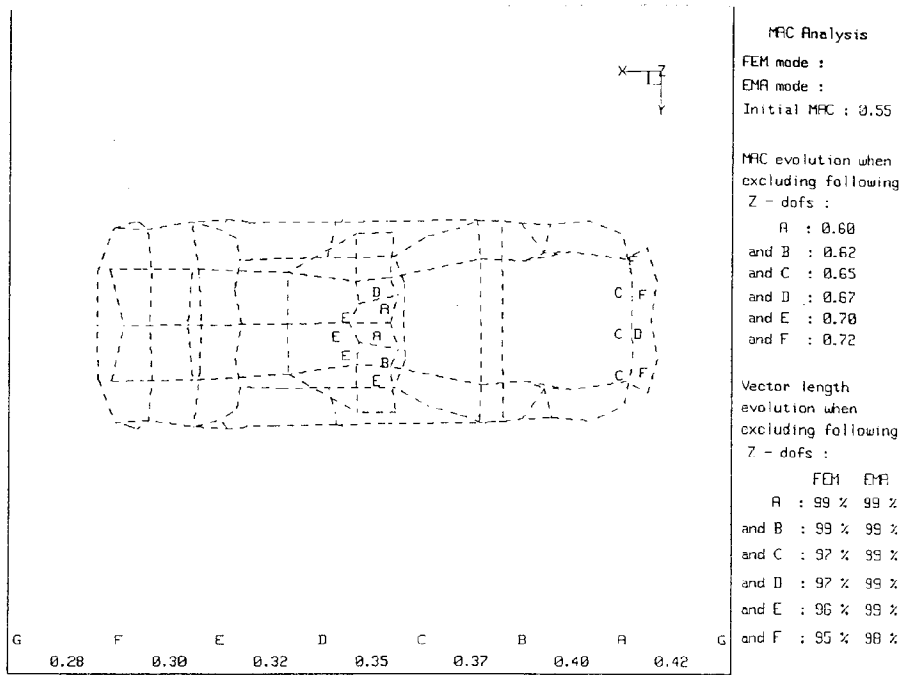
MAC Analysis
FEM mode :
EMA mode :
Initial MAC : 0.55
MAC evolution when excluding following Z - dofs :
A : 0.60
and B : 0.62
and C : 0.65
and D : 0.67
and E : 0.70
and F : 0.72
Vector length evolution when excluding following Z - dofs :
FEM EMA
A : 99 % 99 %
and B : 99 % 99 %
and C : 97 % 99 %
and D : 97 % 99 %
and E : 96 % 99 %
and F : 95 % 98 %
G F E D C B A G
0.28 0.30 0.32 0.35 0.37 0.40 0.42

Fig. 11

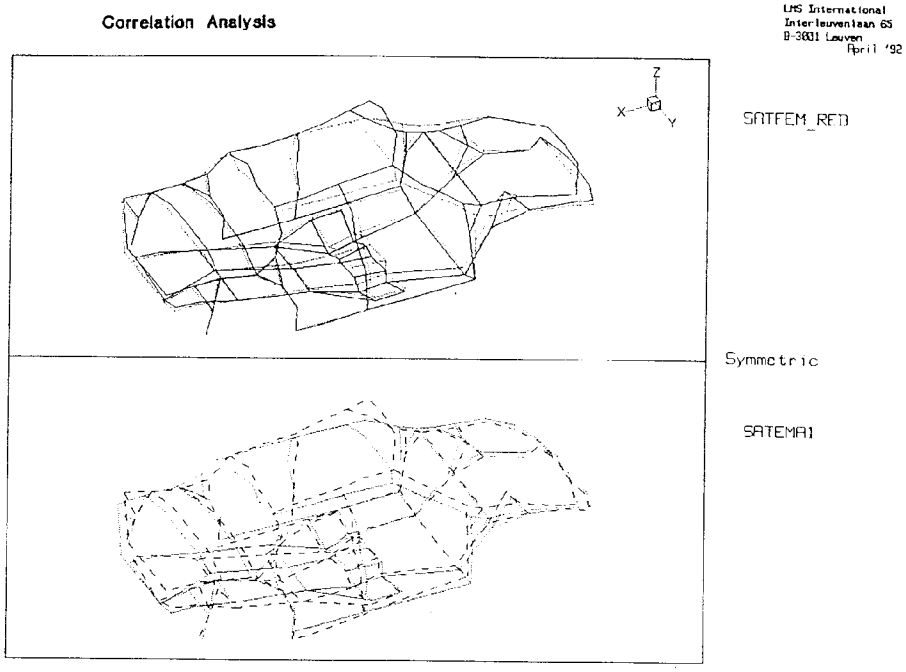
Correlation Analysis
LMS International
Interleuvenlaan 65
B-3001 Leuven
April '92
SATFEM_RED
Symmetric
SATEMA1

Fig. 12

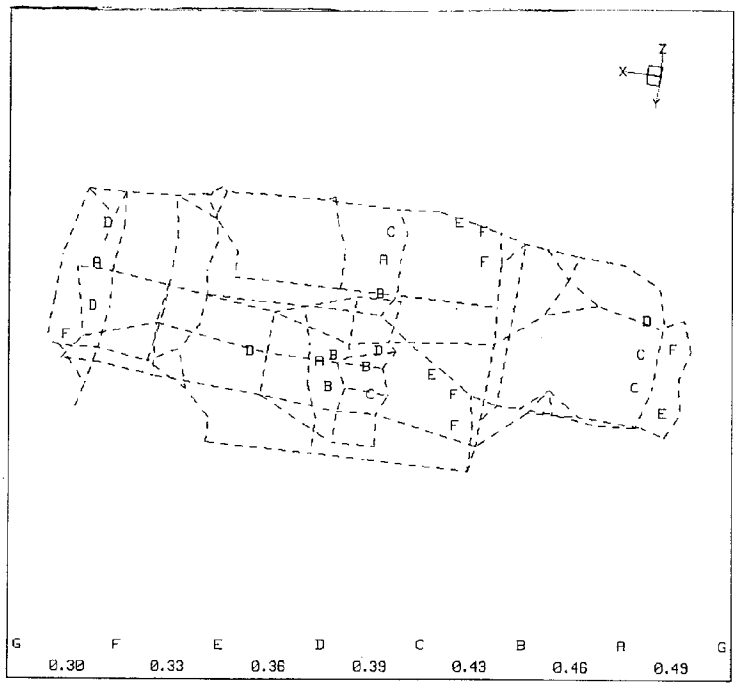
MAC Analysis
FEM mode :
EMA mode :
Initial MAC : 0.50
MAC evolution when excluding following Z - dofs :
A : 0.53
and B : 0.57
and C : 0.60
and D : 0.64
and E : 0.67
and F : 0.70
Vector length evolution when excluding following Z - dofs :
FEM EMA
A : 99 % 99 %
and B : 99 % 96 %
and C : 99 % 90 %
and D : 97 % 87 %
and E : 96 % 85 %
and F : 96 % 81 %
G F E D C B A G
0.30 0.33 0.36 0.39 0.43 0.46 0.49

Fig. 13

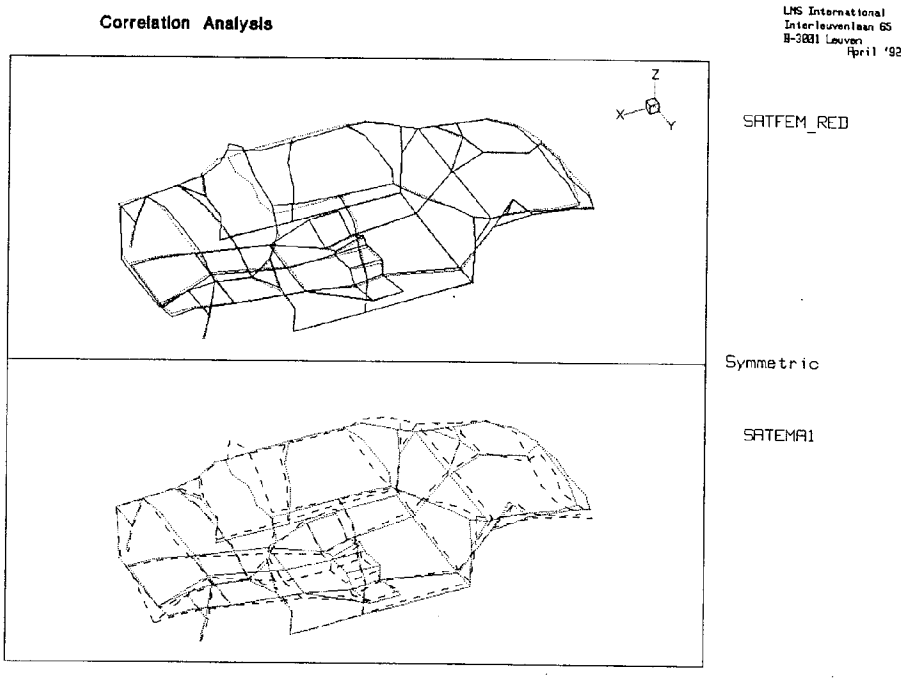
Correlation Analysis
LMS International
Interleuvenlaan 65
B-3001 Leuven
April '92
SATFEM_RED
Symmetric
SATEMA1

Fig. 14

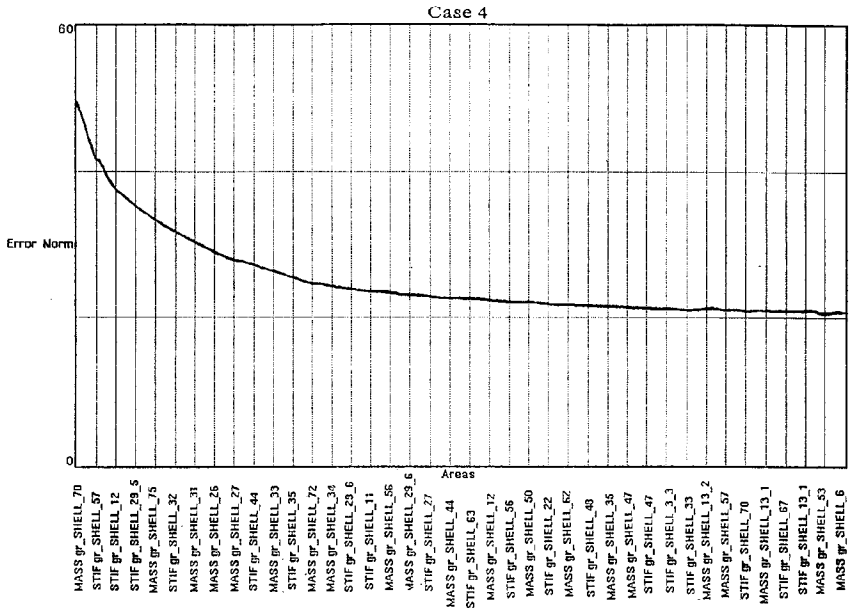

Fig. 15

Fig. 16

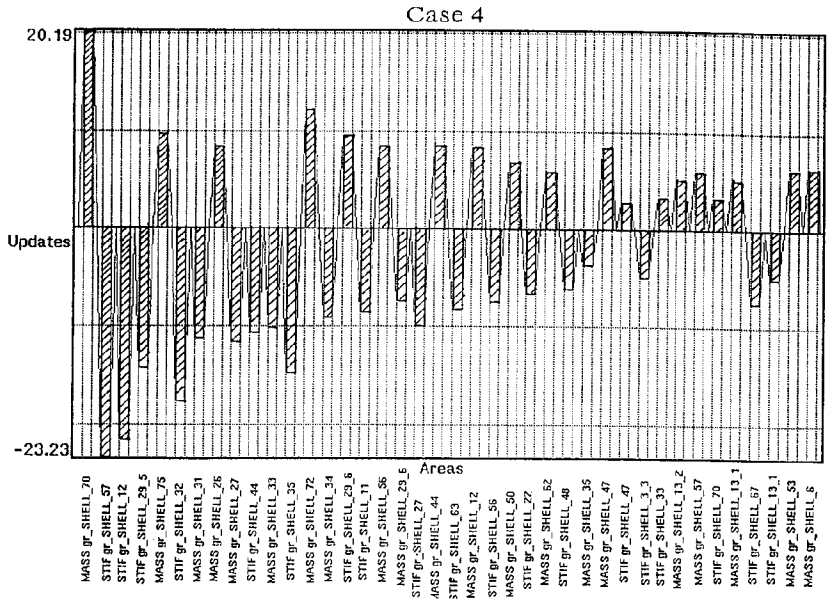

Fig. 17

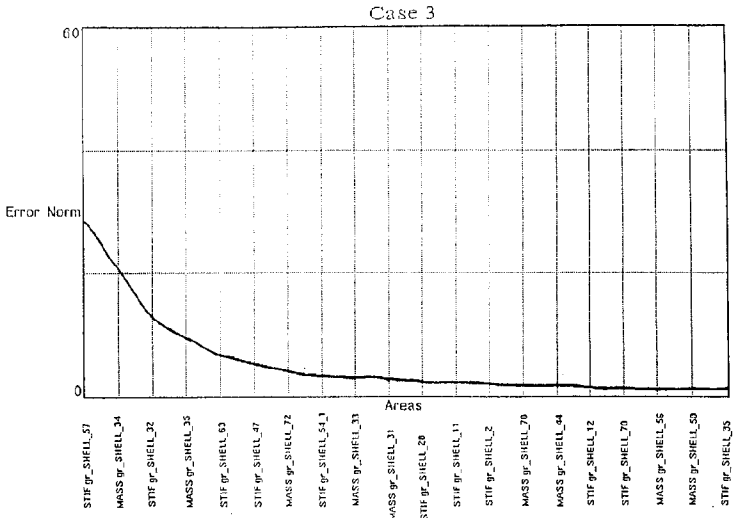

Fig. 18

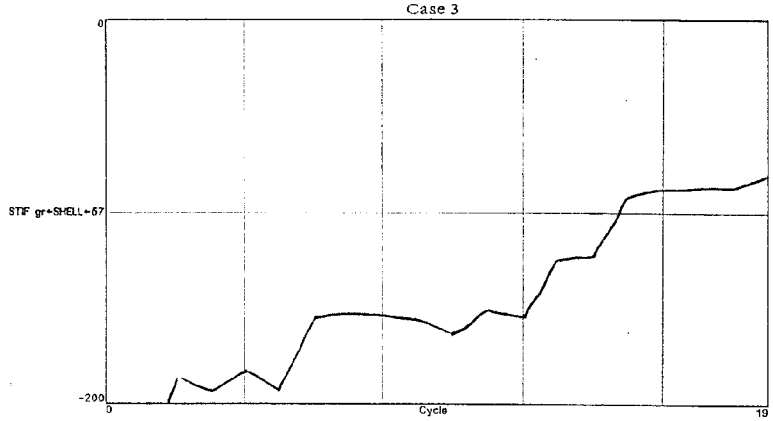

Fig. 19

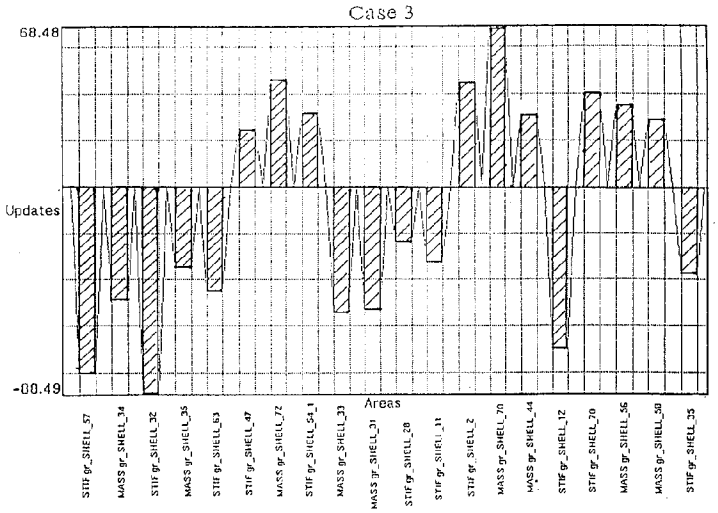

Fig. 20

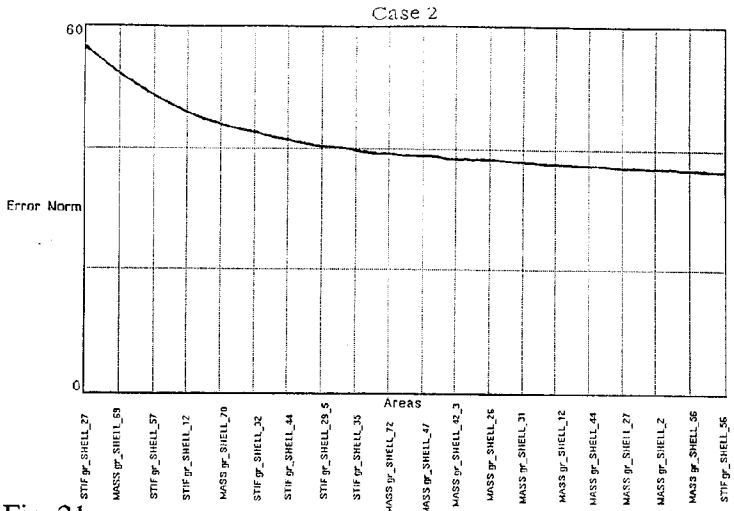

Fig. 21

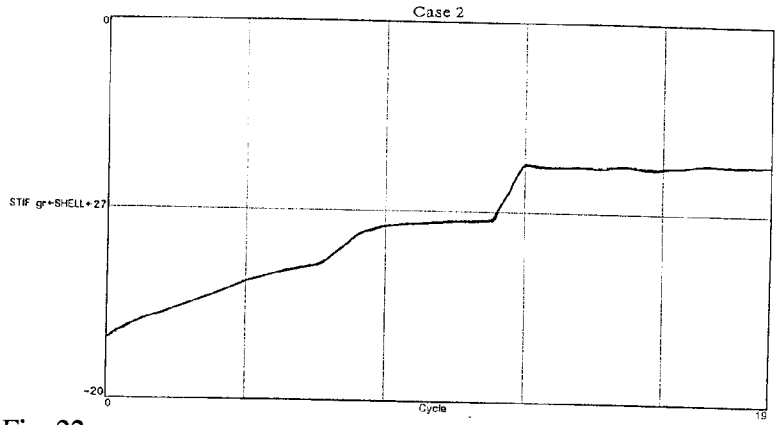

Fig. 22

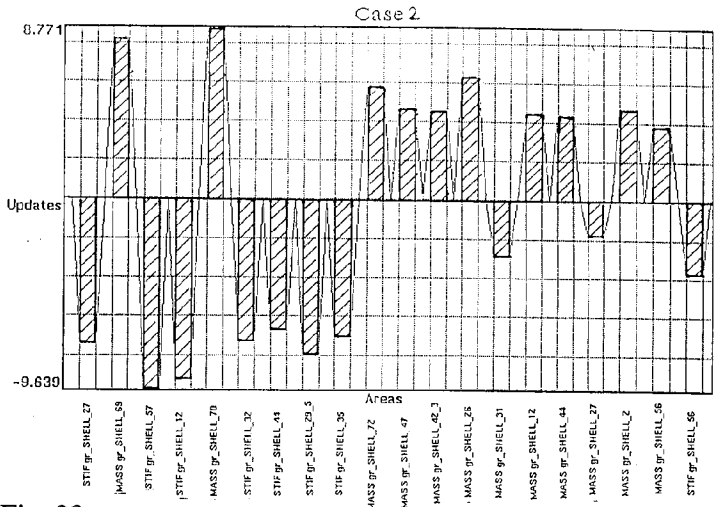

Fig. 23